



## Efficient Synthesis, Spectroscopic and Quantum Chemical Study of 2,3-Dihydrobenzofuran Labelled Two Novel Arylidene Indanones: A Comparative Theoretical Exploration

RAHUL ASHOK SHINDE<sup>1,2</sup>, VISHNU ASHOK ADOLE<sup>1</sup>,  
BAPU SONU JAGDALE<sup>1\*</sup>, THANSING BHAVSING PAWAR<sup>2</sup>,  
BHATU SHIVAJI DESALE<sup>1</sup> and ROHIT SHANKAR SHINDE<sup>1</sup>

<sup>1</sup>Department of Chemistry, Mahatma Gandhi Vidyamandir's Arts, Science and Commerce College  
(Affiliated to Savitribai Phule Pune University, Pune), Manmad-423104

<sup>2</sup>Department of Chemistry, Mahatma Gandhi Vidyamandir's Loknete Vyankatrao Hiray Arts, Science and  
Commerce College Panchavati (Affiliated to SP Pune University, Pune), Nashik-422 003, India.

### Abstract

Indanone and 2,3-dihydrobenzofuran scaffolds are considered as special structures in therapeutic science and explicitly associated with various biologically potent compounds. In the present disclosure, we report the synthesis of two new 2,3-dihydrobenzofuran tethered arylidene indanones via an environmentally adequate and viable protocol. The two compounds revealed in this have been characterized well by analytical methods; proton magnetic resonance (PMR), carbon magnetic resonance (CMR). The Density Functional Theory (DFT) study has been presented for the spectroscopic, structural and quantum correlation between (E)-2-((2,3-dihydrobenzofuran-5-yl)methylene)-2,3-dihydro-1H-inden-1-one (DBDI) and (E)-7-((2,3-dihydrobenzofuran-5-yl)methylene)-1,2,6,7-tetrahydro-8H-indeno[5,4-b]furan-8-one (DBTI). Optimized geometry, frontier molecular orbital, global reactivity descriptors, and thermodynamic parameters have been computed for DBDI and DBTI. DFT/B3LYP method using basis set 6-311++G (d,p) has been employed for the computational study. Mulliken atomic charges are established by using 6-311G (d,p) basis set. Besides, molecular electrostatic potential for DBDI and DBTI is also explored to locate the electrophilic and nucleophilic centres.



### Article History

Received: 04 June 2020

Accepted: 21 July 2020

### Keywords:

DFT, 6-311++G(d,p);  
HOMO-LUMO;  
Molecular Electrostatic  
potential;  
(E)-2-((2,3  
Dihydrobenzofuran-5-yl)  
Methylene)-2,3-Dihydro-  
1H-Inden-1-One;  
(E)-7-((2,3  
Dihydrobenzofuran  
5-yl)Methylene)  
1,2,6,7-Tetrahydro-8H  
Indeno[5,4-b]Furan-8  
one.;

**CONTACT** Bapu Sonu Jagdale ✉ jagdalebs@gmail.com 📍 Department of Chemistry, Mahatma Gandhi Vidyamandir's Loknete  
Vyankatrao Hiray Arts, Science and Commerce College Panchavati (Affiliated to SP Pune University, Pune), Nashik-422 003, India.



© 2020 The Author(s). Published by Oriental Scientific Publishing Company

This is an Open Access article licensed under a Creative Commons Attribution-NonCommercial-ShareAlike 4.0 International License  
Doi: <http://dx.doi.org/10.13005/msri/170207>

### Introduction

In the past few years, research on indanones and related compounds has been explored and they are found to exert an expansive range of biological properties.<sup>1-12</sup> Importantly, they are the exceptionally valuable synthetic equivalents for the synthesis of wide variety of organic compounds having an excellent biologic profile.<sup>13-16</sup> Many bioactive natural products are indanone based molecules. Some noticeable examples (Fig 1) 1-methoxy-6-methyl-3-oxo-2,3-dihydro-1H-indene-4-carbaldehyde (1), isopaucifloral F (2), 4-hydroxy-7-methyl-2,3-dihydro-1H-inden-1-one (3), Paucifloral F (4), Pterisin B (5). These noteworthy naturally derived compounds are known as powerful medicinal agents.<sup>17-22</sup> Donepezil (6) is one of the most important indanone structures which have been proficiently used for the treatment of Alzheimer's disease due to its acetyl cholinesterase inhibitor activity. On the other hand, some eye catching examples of drugs containing dihydrobenzofuran are tasimelteon (9), 1-(2,3-dihydrobenzofuran-5-yl)propan-2-amine (10), 1-(2,3-dihydrobenzofuran-5-yl)-N-methylpropan-2-amine (11) and ((1R,2R)-2-(2,3-dihydrobenzofuran-4-yl)cyclopropyl) methanol (12). The 2-arylidene indanone compounds

have been investigated as potent agents for treatment of Alzheimer's disease, breast cancer and leukaemia, as tubulin depolymerizing agents and many other significant pharmacological applications.<sup>1,23</sup> A medicinally important structure which is being used as sleep inducing agent is Ramelteon (7). Ramelteon binds with MT-1 and MT-2 receptor. It contains a tricyclic synthetic molecule: 1,2,6,7-tetrahydro-8H-indeno[5,4-b]furan-8-one (8). The 2,3-dihydrobenzofuran natural products have pulled in expanding consideration because of their unusual structural highlights and the wide scope of biological activities.<sup>24</sup> The benzofuran and 2,3-disubstituted benzofuran scaffolds are present in countless natural products that exhibit incredible profile of biological activities, such as antimicrobial, antiviral, anti-inflammatory antioxidant, and anticancer activities.<sup>25-29</sup> In recent times, these compounds have been investigated to have various biological activities.<sup>30-37</sup> Henceforth benzofuran containing compounds may be used to design and generate new capacity therapeutic candidates having exceptional importance in the subject of the new drug research.<sup>38-40</sup> The use of green chemistry has been great advantage for the environment.<sup>41-54</sup>

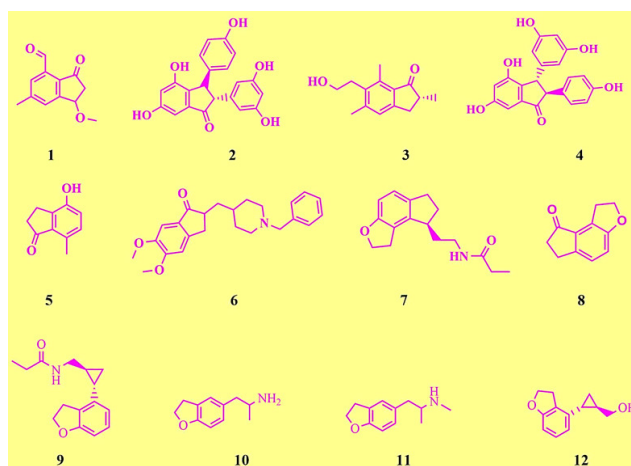


**Fig. 1: Some noticeable examples of indanone and 2,3-dihydrobenzofuran containing biologically active compounds**

Theoretical calculations based on DFT have been successfully explored largely in past few years to determine various structural aspects of synthetically and pharmacologically vital organic motifs.<sup>55-58</sup> DFT/B3LYP method using various basis set has been found to be very crucial for investigating

structural, chemical, and spectroscopic properties of the molecules.<sup>59-63</sup> Considering all mentioned properties and future scope of these molecules, we have designed 2,3-dihydrobenzofuran tethered two important synthetic compounds (scheme 1) and have been explored for the investigation of their structural,

chemical, electronic, thermodynamic and quantum chemical parameters. To the best of our insights, this

is preliminary report on synthesis, characterization and DFT investigation of title molecules.



**Scheme 1** Synthesis of 2,3-dihydrobenzofuran tethered 2-arylidene indanone derivatives

## Methodology

### Materials and Methods

The chemicals with high purity were purchased from local distributor. The chemicals were used as received without any further purification. Melting point was determined in open capillary and uncorrected. <sup>1</sup>H NMR and <sup>13</sup>C NMR spectra were recorded with a Bruker using CDCl<sub>3</sub> as solvent, FT-IR spectra were obtained with potassium bromide pellets. Reaction was monitored by thin-layer chromatography using aluminium sheets with silica gel 60 F254 (Merck).

### Experimental Procedure for the Synthesis of DBDI and DBTI

The synthesis of DBDI and DBTI is presented in Scheme 1. In a typical synthesis procedure, 2,3-dihydrobenzofuran-5-carbaldehyde (I, 10 mmol), 2,3-dihydro-1H-inden-1-one (II, 10 mmol) or 1,2,6,7-tetrahydro-8H-indeno[5,4-b]furan-8-one (III, 8 mmol) was added to a 25 mL flat bottom flask. To this 2 mL 40% NaOH and 5 mL ethanol were added. Then this alkaline mixture was stirred on magnetic stirrer until the formation of desired products (checked by TLC (7:3; hexane: ethyl acetate)). Reaction mass was transferred to a beaker containing ice cold water, then filtered, dried and recrystallized to offer fine yellow crystals of IV or V.

### Computational Details

Density Functional Theory calculations were computed on an Intel (R) Core (TM) i5 computer using Gaussian-03 program package without any constraint on the geometry.<sup>64</sup> The geometry of the title molecules was optimized by DFT/B3LYP method using 6-311++G (d,p) basis set. Optimized

geometry was made using the Gauss View 4.1 molecular visualization program. To investigate the reactive sites of the title compound, the molecular electrostatic potential was computed using the same method. All the calculations were carried out for the optimized structure in the gas phase. Mulliken atomic charges were established by using 6-311G (d,p) basis set.

## Results and Discussion

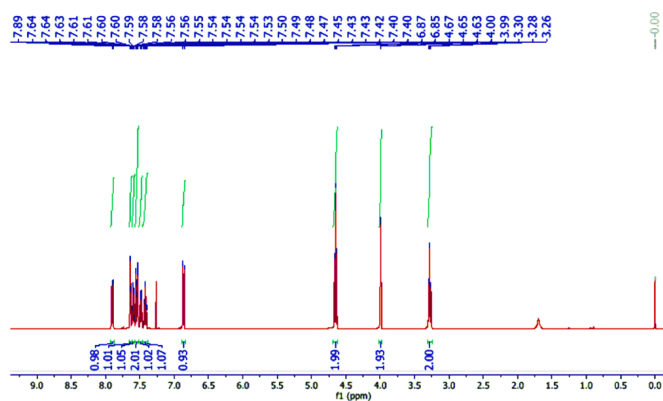
### Spectral Analysis of DBDI and DBTI

The spectral images are given in Fig 2 (13 = <sup>1</sup>H NMR spectrum of DBDI, 14 = <sup>13</sup>C NMR spectrum of DBDI, 15 = <sup>1</sup>H NMR spectrum of DBTI, 16 = <sup>13</sup>C NMR spectrum of DBTI).

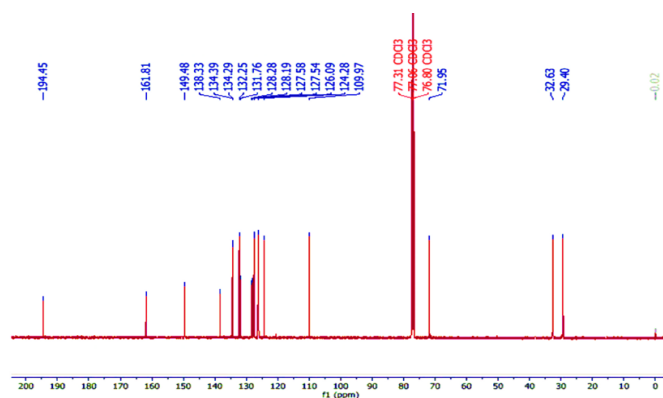
- (E)-2-((2,3-dihydrobenzofuran-5-yl)methylene)-2,3-dihydro-1H-inden-1-one (DBDI) : M.F. C<sub>18</sub>H<sub>14</sub>O<sub>2</sub>; Pale yellow crystals; M.P. 97 °C; <sup>1</sup>H NMR (500 MHz, Chloroform-d) δ - 7.90 (m, 1H), 7.64 (t, J = 2.1 Hz, 1H), 7.60 (td, J = 7.3, 1.2 Hz, 1H), 7.58 – 7.51 (m, 2H), 7.48 (dd, J = 8.3, 1.9 Hz, 1H), 7.47 – 7.38 (m, 1H), 6.86 (d, J = 8.3 Hz, 1H), 4.65 (t, J = 8.7 Hz, 2H), 3.99 (d, J = 2.1 Hz, 2H), 3.28 (t, J = 8.7 Hz, 2H); <sup>13</sup>C NMR (126 MHz, Chloroform-d) δ - 194.45, 161.81, 149.48, 138.33, 134.39, 134.29, 132.25, 131.76, 128.28, 128.19, 127.58, 127.54, 126.09, 124.28, 109.97, 71.95, 32.63, 29.40
- (E)-7-((2,3-dihydrobenzofuran-5-yl)methylene)-1,2,6,7-tetrahydro-8H-indeno[5,4-b]furan-8-one (DBTI) : M.F. C<sub>20</sub>H<sub>16</sub>O<sub>3</sub>; Yellow crystals; M.P. 147°C; IR (KBr, cm<sup>-1</sup>) - 2916.37, 1643.35, 1564.27, 1490.97,

1427.32, 1328.95, 1280.73;  $^1\text{H}$  NMR (500 MHz, Chloroform- $d$ )  $\delta$  7.56 (d,  $J = 2.2$  Hz, 1H), 7.52 (s, 1H), 7.47 (dd,  $J = 8.3, 1.9$  Hz, 1H), 7.28 (s, 1H), 7.02 (d,  $J = 8.0$  Hz, 1H), 6.86 (d,  $J = 8.3$  Hz, 1H), 4.67 (dt,  $J = 14.6, 8.8$  Hz, 4H), 3.93 (d,  $J = 2.0$  Hz, 2H), 3.56 (t,

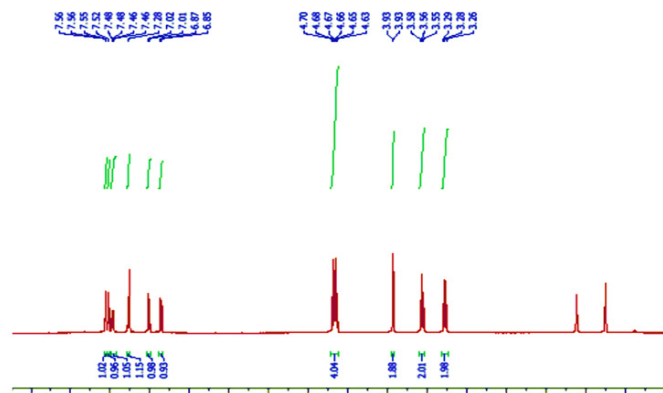
$J = 8.9$  Hz, 2H), 3.28 (t,  $J = 8.7$  Hz, 2H);  $^{13}\text{C}$  NMR (126 MHz, Chloroform- $d$ )  $\delta$  - 194.69, 161.73, 160.45, 141.39, 134.86, 133.83, 132.88, 132.20, 128.34, 128.13, 127.51, 125.03, 124.56, 115.13, 109.93, 72.44, 71.93, 32.23, 29.41, 28.54



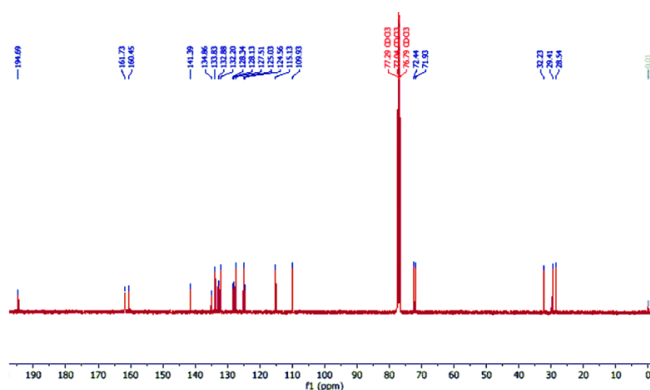
13



14



15

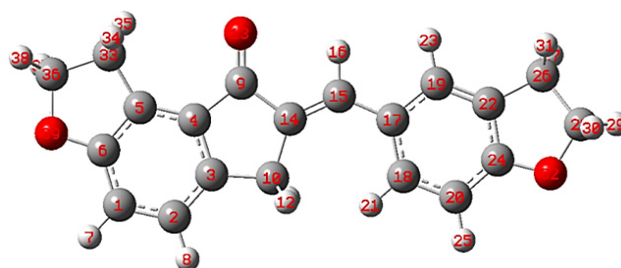


16

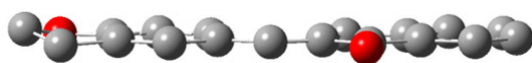
**Fig. 2: Spectral images of the synthesized compounds (13 =  $^1\text{H}$  NMR spectrum of DBDI, 14 =  $^{13}\text{C}$  NMR spectrum of DBDI, 15 =  $^1\text{H}$  NMR spectrum of DBTI, and 16 =  $^{13}\text{C}$  NMR spectrum of DBTI)**



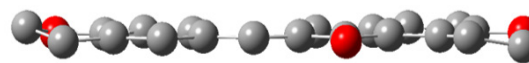
17



18



19



20

**Fig. 3: Optimized molecular structures of DBDI (17), DBTI (18), side view of DBDI (19), side view of DBTI (20)**

Note: Hydrogen atoms are omitted in structures 11 and 12 for clarity

### Computational Study

The optimized molecular structure of title molecules is depicted in Fig 3. Molecular structures 17 and 18

represent optimized geometrical structures for DBDI and DBTI respectively. The optimized molecular geometry provides good deal of information about

the spatial orientation of various atoms in a molecule. From optimized molecular structures, it can be easily seen that both DBDI and DBTI possess C1 point group symmetry due to overall asymmetry of the molecules. Furthermore, it is evident that both the molecules contain non-planar dihydrofuran ring [Fig 3 (19 and 20)]. The non-planarity of dihydrofuran can be attributed to CH<sub>2</sub> group (adjacent to oxygen atom) which is either above or below the plane. Due to this fact, both the molecules lack molecular plane ( $\sigma_h$ ). It can also be seen that remaining skeleton of these molecules are in perfect planar position

and therefore can have extended conjugation. This information is very much useful for the determination of various spectroscopic entities. The optimized geometrical parameters like bond lengths and bond angles of DBDI and DBTI are presented in Table 1A and 1B. The C9-O13 bond is 1.2195 Å in DBDI and C9- 1.2216 Å in DBTI. The olefinic C14-C15 bond is 1.3489 Å and 1.3491 Å in DBDI and DBTI molecules respectively. Other bond lengths are also in good agreement with the optimized structures. Bond angle data of both molecules are also in good agreement.

**Table 1A: Optimized geometrical parameters of DBDI by DFT/ B3LYP with 6-311++G(d,p) basis set**

Bond lengths (Å)					
C1-C2	1.3955	C9-C14	1.4968	C20-C24	1.39
C1-C6	1.4016	C10-H11	1.0966	C22-C25	1.0828
C1-H7	1.0846	C10-H12	1.0966	C22-C24	1.396
C2-C3	1.392	C10-H14	1.5142	C22-C28	1.5123
C2-H8	1.0852	C14-C15	1.3489	C24-O34	1.3588
C3-C4	1.3967	C15-H16	1.0892	C28-H29	1.0949
C3- C10	1.5162	C15-C17	1.4554	C28-C30	1.5454
C4-C5	1.3949	C17-C18	1.4111	C28-H33	1.0919
C4-C9	1.485	C17-C19	1.4153	C30-H31	1.089
C5- C6	1.3908	C18-C20	1.3917	C30-H32	1.0935
C5- H26	1.0841	C18-H21	1.0803	C30-O34	1.4575
C6- H27	1.0841	C19-C22	1.3806	-	-
C9-O13	1.2195	C19-H23	1.0852	-	-
Bond angles (°)					
C2-C1-C6	121.0843	C3-C10-H12	111.0202	C24-C20-H25	120.7525
C2-C1-H7	119.5183	C3-C10-C14	103.716	C19-C22-C24	119.7843
C6-C1-H7	119.3974	H11-C10-H12	106.8518	C29-C22-C28	132.2832
C1-C2-C3	118.7113	C11-C10-C14	112.1608	C24-C22-C28	107.8768
C1-C2-H8	120.2384	H12-C10-C14	112.1657	C20-C24-C22	121.8831
C3-C2-H8	121.0502	C9-C14-C10	108.9035	C20-C24-O34	124.6712
C2-C3-C4	119.9694	C9-C14-C15	119.6675	C22-C24-O34	113.443
C2-C3-C10	128.8339	C10-C14-C15	131.4291	C22-C28-H29	110.9107
C4-C3-C10	111.1967	C14-C15-H16	113.501	C22-C28-C30	101.3765
C3-C4-C5	121.5946	C14-C15-C17	131.9157	C22-C28-C33	113.4248
C3-C4-C9	109.8763	H16-C15-C17	114.5833	H29-C28-C30	111.6154
C5-C4-C9	128.529	C15-C17-C18	124.5419	H29-C28-H33	107.733
C4-C5-26	118.3789	C15-C17-C19	117.4689	C30-C28-H33	111.7831
C4-C5-C26	119.9287	C18-C17-C19	117.9891	C28-C30-C31	114.1679
C6-C5-C26	121.6924	C17-C18-C20	122.1142	C28-C30-H32	111.7492
C1-C6-C5	120.2615	C17-C18-H21	119.8067	C28-C30-O34	106.6458

C1-C6-C27	119.5862	C20-C18-H21	118.0781	H31-C30-H32	109.2705
C5-C6-C27	120.1523	C17-C19-C22	120.4148	H31-C30-O34	107.3237
C4-C9-O13	126.7014	C17-C19-H23	119.0694	H32-C30-O34	107.3357
C4-C9-H14	106.3076	C22-C19-H23	120.5157	C24-O34-C30	107.5144
O13-C9-H14	126.991	C18-C20-C24	117.8125	-	-
C3-C10-H11	111.0122	C18-C20-H25	121.4346	-	-

**Table 1B: Optimized geometrical parameters of DBTI by DFT/ B3LYP with 6-311++G(d,p) basis set**

Bond lengths (Å)					
C1-C2	1.3997	C10-H12	1.0967	C24-H32	1.359
C1-C6	1.3939	C10-C14	1.5147	C26-H27	1.095
C1-H7	1.0832	C14-C15	1.3491	C26-C28	1.5455
C2-C3	1.3921	C15-H16	1.0893	C26-H31	1.0919
C2-H8	1.0851	C15-C17	1.4554	C28-H29	1.089
C3-C4	1.4029	C17-C18	1.4112	C28-H30	1.0936
C3-C10	1.5171	C17-C19	1.4152	C28-H32	1.4572
C4-C5	1.3896	C18-C20	1.3917	C33-H34	1.0948
C4-C9	1.4812	C18-H21	1.0803	C33-H35	1.0907
C5-C6	1.3917	C19-C22	1.3806	C33-C36	1.546
C5-C33	1.5076	C19-H23	1.0852	C36-H37	1.094
C6-O39	1.3649	C20-C24	1.39	C36-H38	1.0892
C9-O13	1.2216	C20-H25	1.0828	C36-O39	1.4579
C9-C14	1.4959	C22-C24	1.396	-	-
C10-H11	1.0969	C22-C26	1.5123	-	-
Bond angles (°)					
C2-C1-C6	118.5211	H12-C10-C14	111.9372	C22-C26-C28	101.3739
C2-C1-H7	121.2674	C9-C14-C10	108.9942	C22-C26-H31	113.4203
C6-C1-H7	120.2114	C9-C14-C15	119.5279	H27-C26-C28	111.6235
C1-C2-C3	119.9287	C10-C14-C15	131.4776	H27-C26-H31	107.7282
C1-C2-H8	119.3749	C14-C15-H16	113.5279	C28-C26-H31	111.775
C3-C2-H8	120.6958	C14-C15-C17	131.868	C26-C28-H29	114.1682
C2-C3-C4	120.3155	H16-C15-C17	114.604	C26-C28-H30	111.7328
C2-C3-C10	128.7497	C15-C17-C18	124.5193	C26-C28-O32	106.6493
C4-C3-C10	110.9348	C15-C17-C19	117.4754	H29-C28-H30	109.266
C3-C4-C5	120.4952	C18-C17-C19	118.0053	H29-C28-O32	107.3348
C3-C4-C9	109.9704	C17-C18-C20	122.0958	H30-C28-O32	107.3437
C5-C4-C9	129.5343	C17-C18-H21	119.7491	C24-O32-C28	107.5129
C4-C5-C6	118.2297	C20-C18-H21	118.1546	C5-C33-H34	110.6631
C4-C5-C33	133.2551	C17-C19-C22	120.4133	C5-C33-H35	113.1536
C6-C5-C33	108.4696	C17-C19-H23	119.0843	C5-C33-C36	101.1394
C1-C6-C5	122.5085	C22-C19-H23	120.5024	H34-C33-H35	107.1137
C1-C6-O39	124.3126	C18-C20-C24	117.8164	H34-C33-C36	112.2093
C5-C6-O39	113.175	C18-C20-H25	121.4388	H35-C33-C36	112.6213
C4-C9-O13	126.6343	C24-C20-H25	120.7445	C33-C36-H37	111.603
C4-C9-C14	106.3681	C19-C22-C24	119.7754	C33-C36-H38	114.1268
O13-C9-C14	126.9976	C19-C22-C26	132.2866	C33-C36-O39	106.8638



can undergo nucleophilic attack easily. The molecule DBDI involves more electron transfer than DBTI as predicted by  $\Delta N_{\max}$ ; however it requires little bit more energy than DBTI.

**Table 2: Electronic Parameters**

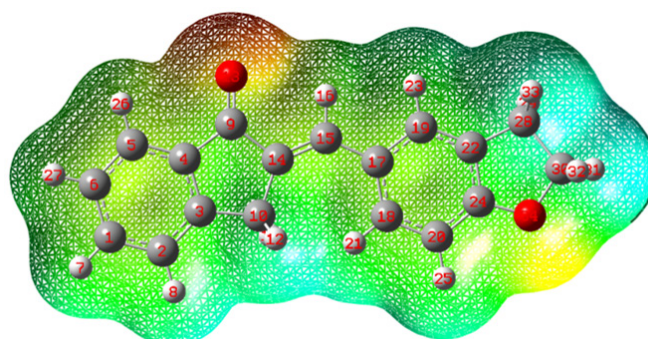
Entry	$E_{\text{Total}}$ (a.u.)	$E_{\text{HOMO}}$ (eV)	$E_{\text{LUMO}}$ (eV)	$\Delta E$ (eV)	I(eV)	A(eV)
DBDI	-845.0077	-5.9698	-2.2680	3.7018	5.9698	2.2680
DBTI	-997.6827	-5.9434	-2.2536	3.6898	5.9434	2.2536

Note: I =  $-E_{\text{HOMO}}$  & A =  $-E_{\text{LUMO}}$

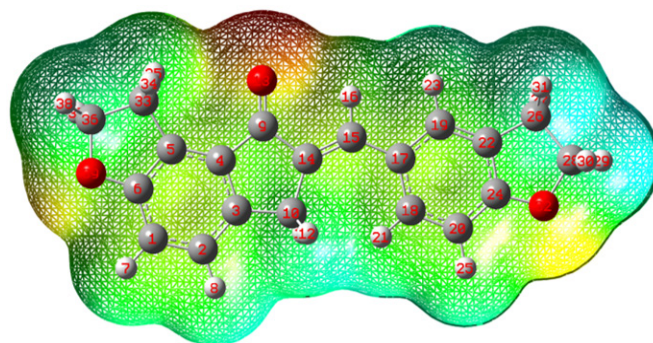
**Table 3: Quantum Chemical Parameters**

Entry	$\chi$ (eV)	$\eta$ (eV)	$\sigma$ (eV <sup>-1</sup> )	$\omega$ (eV)	Pi(eV)	$\Delta N_{\max}$ (eV)	Dipole moment (Debye)
DBDI	4.1189	1.8509	0.5403	4.5830	-4.1189	2.2553	3.5520
DBTI	4.0985	1.8449	0.5420	4.5525	-4.0985	2.2215	3.0116

Note:  $\chi = (I + A)/2$ ;  $\eta = (I - A)/2$ ;  $\sigma = 1/\eta$ ;  $\omega = \text{Pi}/2\eta$ ;  $\text{Pi} = -\chi$ ;  $\Delta N_{\max} = -\text{Pi}/\eta$



23



24

**Fig. 5: Molecular electrostatic potentials; 23 for DBDI and 24 for DBTI**

The MEP plots are displayed in Fig 5. The properties like dipole moment, electronegativity, partial charges and chemical reactivity of any molecule can be correlated with the aid of molecular electrostatic potential. The molecular electrostatic potential is a total charge distribution of a molecule space. The regions of positive, negative and neutral potentials are indicated by different colours. Red suggests a zone of negative electrostatic potential and the white zone of positive electrostatic potential. In the present case, it can be observed that negative electrostatic potential lies over oxygen atom in both

DBDI and DBTI. On the other hand, the positive electrostatic potential is situated over hydrogen atoms of two aromatic rings. The blue part indicates zero electrostatic potential and it is mainly located over hydrogen atoms of dihydrofuran ring in both DBDI and DBTI. The molecule DBTI has less positive electrostatic potential than DBDI. This is due to the presence of extra dihydrofuran ring in DBTI. These zones of various electrostatic potential can give valuable data in regards to various sorts of intermolecular interactions and hence one can foresee the chemical behaviour of the molecule.

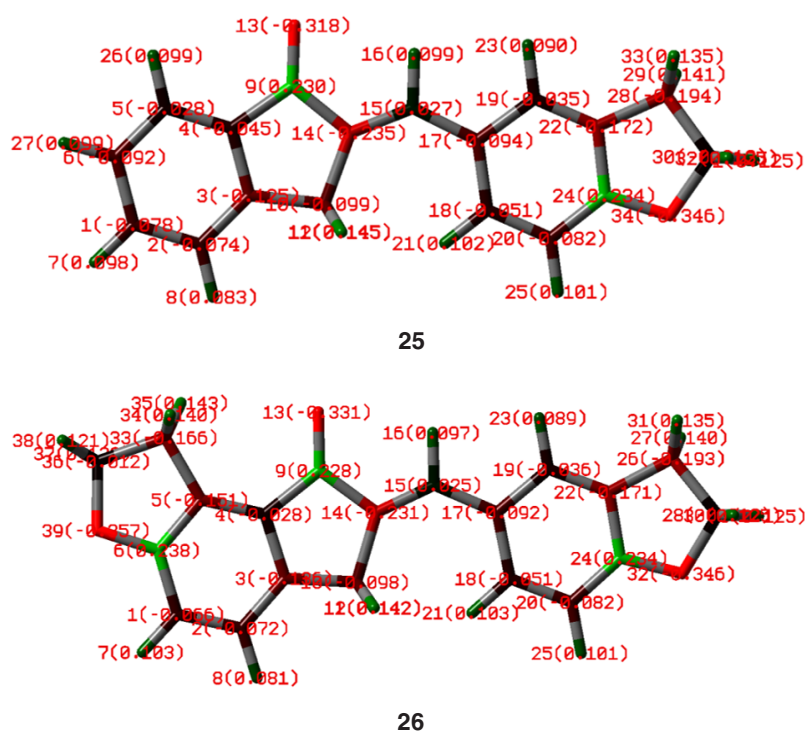


**Fig. 6: Mulliken atomic charges; 25 for DBDI and 26 for DBTI**

The different thermodynamic properties were computed from the theoretical vibrational frequencies and are presented in Table 6. The thermodynamic data disclosed in this could provide valuable insights to the other thermodynamic parameters. In present investigation, the theoretical thermodynamic calculations based on vibrational data provided valuable insights on thermodynamic stability of the title molecules. Our study reveals that the molecule DBTI is thermodynamically more stable than DBDI. Moreover DBTI possesses more degree of translational, rotational and vibrational freedom

as compared to DBDI. Also, it has higher value of heat capacity. Mulliken atomic charges of DBDI and DBTI are presented in Table 4 and Fig 6. Mulliken atomic charges give important information regarding electropositive and electronegative nature of atoms. All hydrogen atoms are electropositive as they are attached to atoms having more electronegativity than hydrogen. Out of two oxygen atoms in DBDI molecule, 34O is more negative with Mulliken atomic charge value of -0.346342. On the other hand, 39O is the most negative with Mulliken atomic charge value of -0.357181.

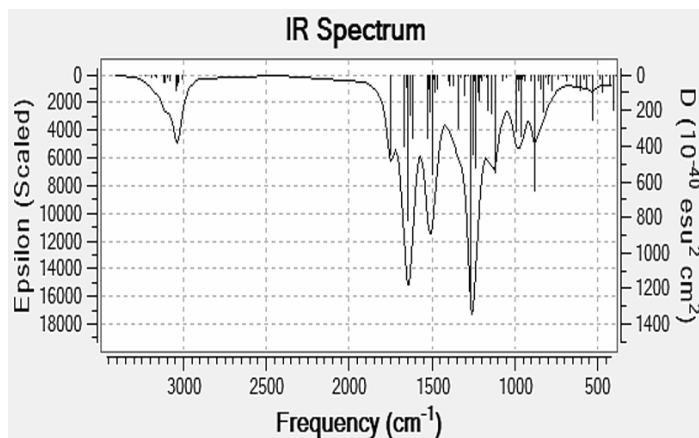
Table 4: Mulliken atomic charges

DBDI		DBTI	
Atom	Charge	Atom	Charge
1 C	-0.077564	1 C	-0.066467
2 C	-0.073918	2 C	-0.071827
3 C	-0.124734	3 C	-0.136440
4 C	-0.045291	4 C	-0.028203
5 C	-0.027585	5 C	-0.151259
6 C	-0.091625	6 C	0.237673
7 H	0.098412	7 H	0.103104
8 H	0.083048	8 H	0.081455
9 C	0.229546	9 C	0.228244
10 C	-0.099451	10 C	-0.097862
11 H	0.144775	11 H	0.141638
12 H	0.144745	12 H	0.141771
13 O	-0.317630	13 O	-0.330787
14 C	-0.235269	14 C	-0.230793
15 C	0.027322	15 C	0.025347
16 H	0.098993	16 H	0.097262
17 C	-0.093882	17 C	-0.092018
18 C	-0.050912	18 C	-0.050598
19 C	-0.034868	19 C	-0.035806
20 C	-0.081547	20 C	-0.081903
21 H	0.101597	21 H	0.102766
22 C	-0.171504	22 C	-0.171159
23 H	0.089924	23 H	0.089055
24 C	0.233928	24 C	0.233868
25 H	0.101132	25 H	0.101140
26 H	0.099328	26 C	-0.193460
27 H	0.098860	27 H	0.140271
28 C	-0.193507	28 C	-0.012403
29 H	0.140606	29 H	0.125239
30 C	-0.012580	30 H	0.125046
31 H	0.125473	31 H	0.134920
32 H	0.125273	32 O	-0.346495
33 H	0.135247	33 C	-0.165668
34 O	-0.346342	34 H	0.139763
-	-	35 H	0.143083
-	-	36 C	-0.012170
-	-	37 H	0.120278
-	-	38 H	0.120579
-	-	39 O	-0.357181

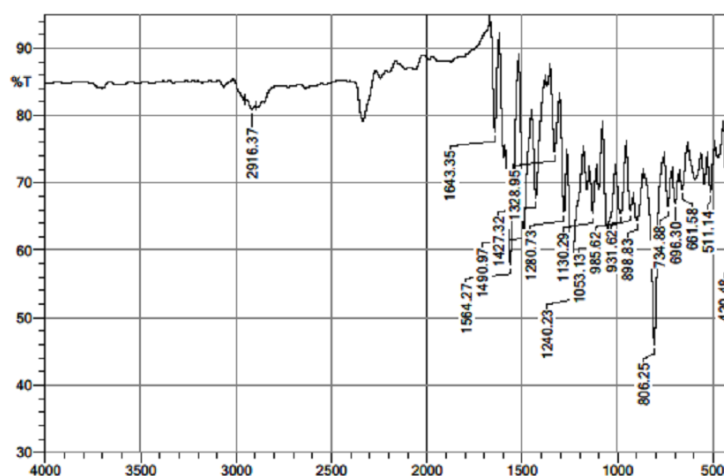
Table 5: Thermodynamic properties

Parameter	DBDI	DBTI
E total (kcal mol <sup>-1</sup> )	179.528	205.961
Translational	0.889	0.889
Rotational	0.889	0.889
Vibrational	177.751	204.183
Heat Capacity at constant volume, Cv (cal mol <sup>-1</sup> K <sup>-1</sup> )	61.812	71.567
Translational	2.981	2.981
Rotational	2.981	2.981
Vibrational	55.85	65.605
Total entropy S (cal mol <sup>-1</sup> K <sup>-1</sup> )	128.401	140.894
Translational	42.59	43.033
Rotational	34.076	34.964
Vibrational	51.735	62.897
Zero point Vibrational Energy Ev0 (kcal mol <sup>-1</sup> )	169.82521	194.65241
Rotational constants	1.2333834	1.0102184
	0.1314400	0.0921864
	0.1190901	0.0847426
E (RB3LYP) (a.u.)	-845.0077	-997.6827

The theoretical IR spectrum of DBTI is computed at DFT/B3LYP method using 6-311++G (d,p) basis set. The theoretical and experimental IR spectra are Figure 7A and Figure 7B respectively. There are total 111 fundamental modes of vibrations as per 3N-6 formula. The important experimental IR vibrations are 2916.37, 1643.35, 1564.27, 1490.97, and 1427.32 cm<sup>-1</sup>. The 2916.37 cm<sup>-1</sup> is due to the asymmetric C-H vibrations. The similar vibration is at 2917.36 cm<sup>-1</sup> in the theoretical spectrum. The C=O frequency is appeared at 1643.35 cm<sup>-1</sup>. The carbonyl stretching is located at 1679.68 cm<sup>-1</sup> in the simulated IR spectrum. The C=C vibrations are 1564.27, 1490.97, and 1427.32 cm<sup>-1</sup>. There is good agreement between the theoretical and experimental IR spectra.



A



B

Fig. 7 A: Theoretical IR B. Experimental IR

### Conclusions

In the present research work, DFT/B3LYP method at 6-311++G (d,p) basis set has been used for the exploration of various important structural, electronic and quantum chemical parameters of title molecules. An elaborative correlation among DBDI and DBTI has been presented. The properties like the HOMO-LUMO energy gap, charge transfer phenomenon, molecular electrostatic potential, and global reactivity descriptors have been explored using the same level of method. Additionally, important thermodynamic statistics have been computed and these two molecules have been compared based on this data to elucidate their thermodynamic behaviour. The theoretical analysis of the two title compounds furnished the following results. Both

DBDI and DBTI possess C1 point group symmetry due to the overall asymmetry of the molecules. The molecule DBDI possesses a higher dipole moment than the molecule DBTI. The HOMO-LUMO gap in DBDI is 3.7018 eV and in DBTI is 3.6898 eV. The MEP analysis suggests that the molecule DBTI has less positive electrostatic potential than DBDI. Thermochemical data reveals that the molecule DBTI is thermodynamically more stable than DBDI. Moreover, DBTI possesses more degree of translational, rotational, and vibrational freedom as compared to DBDI. The 39O is the most negative with Mulliken atomic charge value of -0.35718 in the DBTI molecule whereas 34O is more negative with Mulliken atomic charge value of -0.346342 in DBDI.

**Acknowledgments**

Authors acknowledge Central instrumentation facility, Savitribai Phule Pune University, Pune for NMR and Mass spectral analysis. Authors also would like to thank Lokenete Vyankatrao Hiray Arts, Science and Commerce College Panchavati, Nashik and Arts, Science and Commerce College, Manmad for permission and providing necessary research facilities. Authors would like to express their sincere and humble gratitude to Prof. Arun B. Sawant for Gaussian study. Dr. Aapoorva Hiray, Coordinator, MG

Vidyamandir institute, is gratefully acknowledged for Gaussian package.

**Funding**

We have not received any kind of fund for the research work.

**Conflict of Interest**

Authors declared that they do not have any conflict of interest regarding this research article.

**References**

- Patil, S.A., Patil, R. and Patil, S.A., 2017. Recent developments in biological activities of indanones. *European journal of medicinal chemistry*, 138, pp.182-198.
- Menezes, J.C., 2017. Arylidene indanone scaffold: medicinal chemistry and structure–activity relationship view. *RSC advances*, 7(15), pp.9357-9372.
- Singh, A., Fatima, K., Singh, A., Behl, A., Minto, M.J., Hasanain, M., Ashraf, R., Luqman, S., Shanker, K., Mondhe, D.M. and Sarkar, J., 2015. Anticancer activity and toxicity profiles of 2-benzylidene indanone lead molecule. *European Journal of Pharmaceutical Sciences*, 76, pp.57-67.
- Tang, M.L., Zhong, C., Liu, Z.Y., Peng, P., Liu, X.H. and Sun, X., 2016. Discovery of novel sesquiterpene indanone analogues as potent anti-inflammatory agents. *European journal of medicinal chemistry*, 113, pp.63-74.
- Panara, M.R., Greco, A., Santini, G., Sciulli, M.G., Rotondo, M.T., Padovano, R., di Giamberardino, M., Cipollone, F., Cuccurullo, F., Patrono, C. and Patrignani, P., 1995. Effects of the novel anti-inflammatory compounds, N-[2-(cyclohexyloxy)-4-nitrophenyl] methanesulphonamide (NS-398) and 5-methanesulphonamido-6-(2,4-difluorothiophenyl)-1-indanone (L-745, 337), on the cyclo-oxygenase activity of human blood prostaglandin endoperoxide synthases. *British journal of pharmacology*, 116(5), pp.2429-2434.
- Gómez, N., Santos, D., Vázquez, R., Suescun, L., Mombrú, Á., Vermeulen, M., Finkielstein, L., Shayo, C., Moglioni, A., Gambino, D. and Davio, C., 2011. Synthesis, Structural Characterization, and Pro-apoptotic Activity of 1-Indanone Thiosemicarbazone Platinum (II) and Palladium (II) Complexes: Potential as Antileukemic Agents. *ChemMedChem*, 6(8), pp.1485-1494.
- Saravanan, V.S., Selvan, P.S., Gopal, N. and Gupta, J.K., 2006. Synthesis and pharmacological evaluation of some indanone-3-acetic acid derivatives. *Asian Journal of Chemistry*, 18(4), p.2597.
- Li, C.S., Black, W.C., Chan, C.C., Ford-Hutchinson, A.W., Gauthier, J.Y., Gordon, R., Guay, D., Kargman, S. and Lau, C.K., 1995. Cyclooxygenase-2 inhibitors. Synthesis and pharmacological activities of 5-methanesulfonamido-1-indanone derivatives. *Journal of medicinal chemistry*, 38(25), pp.4897-4905.
- Hammen, Philip D., and George M. Milne Jr. "2-Aminomethyleneindanone analgesic agents." U.S. Patent 4,164,514, issued August 14, 1979.
- Sheng, R., Xu, Y., Hu, C., Zhang, J., Lin, X., Li, J., Yang, B., He, Q. and Hu, Y., 2009. Design, synthesis and AChE inhibitory activity of indanone and aurone derivatives. *European journal of medicinal chemistry*, 44(1), pp.7-17.
- Albrecht, R., Kessler, H.J. and Schroder, E., Bayer Pharma AG, 1972. *Antimicrobial indanones*. U.S. Patent 3,671,520.
- Omran, Z., Cailly, T., Lescot, E., Sopkova-de Oliveira Santos, J., Agondanou, J.H., Lisowski, V., Fabis, F., Godard, A.M., Stiebing, S., Le

- Flem, G. and Boulouard, M., 2005. Synthesis and biological evaluation as AChE inhibitors of new indanones and thiaindanones related to donepezil. *European journal of medicinal chemistry*, 40(12), pp.1222-1245.
13. Herzog, M.N., Chien, J.C. and Rausch, M.D., 2002. Novel 2-indenyl ansa-zirconocenes for the polymerization of  $\alpha$ -olefins. *Journal of organometallic chemistry*, 654(1-2), pp.29-35.
14. DJ, K., 2007. Hamel E. Jung MK. Flynn BL. *Bioorg. Med. Chem*, 15, p.3290.
15. Leoni, L.M., Hamel, E., Genini, D., Shih, H., Carrera, C.J., Cottam, H.B. and Carson, D.A., 2000. Indanocine, a microtubule-binding indanone and a selective inducer of apoptosis in multidrug-resistant cancer cells. *Journal of the National Cancer Institute*, 92(3), pp.217-224.
16. Patel, V., Bhatt, N., Bhatt, P. and Joshi, H.D., 2014. Synthesis and pharmacological evaluation of novel 1-(piperidin-4-yl)-1H-benzo [d] imidazol-2 (3H)-one derivatives as potential antimicrobial agents. *Medicinal Chemistry Research*, 23(4), pp.2133-2139.
17. Sheridan, H., Frankish, N. and Farrell, R., 1999. Synthesis and antispasmodic activity of analogues of natural pterosins. *European journal of medicinal chemistry*, 34(11), pp.953-966.
18. Syrchina, A.I. and Semenov, A.A., 1982. Natural indanones. *Chemistry of Natural Compounds*, 18(1), pp.1-11.
19. Jaki, B., Heilmann, J. and Sticher, O., 2000. New Antibacterial Metabolites from the Cyanobacterium *Nostoc commune* (EAWAG 122b). *Journal of Natural Products*, 63(9), pp.1283-1285.
20. Nagle, D.G., Zhou, Y.D., Park, P.U., Paul, V.J., Rajbhandari, I., Duncan, C.J. and Pasco, D.S., 2000. A New Indanone from the Marine Cyanobacterium *Lyngbya majuscula* That Inhibits Hypoxia-Induced Activation of the VEGF Promoter in Hep3B Cells. *Journal of natural products*, 63(10), pp.1431-1433.
21. Kovganko, N.V., Kashkan, Z.N. and Krivenok, S.N., 2004. Bioactive Compounds of the Flora of Belarus. 4. Pterosins A and B from *Pteridium aquilinum*. *Chemistry of natural compounds*, 40(3).
22. Ge, X., Ye, G., Li, P., Tang, W.J., Gao, J.L. and Zhao, W.M., 2008. Cytotoxic diterpenoids and sesquiterpenoids from *Pteris multifida*. *Journal of natural products*, 71(2), pp.227-231.
23. Adole, V.A., Pawar, T.B. and Jagdale, B.S., 2019. Aqua-mediated rapid and benign synthesis of 1,2,6,7-tetrahydro-8H-indeno [5,4-b] furan-8-one-appended novel 2-arylidene indanones of pharmacological interest at ambient temperature. *Journal of the Chinese Chemical Society*, 67:306-315.
24. Chen, Z., Pitchakuntla, M. and Jia, Y., 2019. Synthetic approaches to natural products containing 2,3-dihydrobenzofuran skeleton. *Natural product reports*, 36(4), pp.666-690.
25. Dawood, K.M., 2013. Benzofuran derivatives: a patent review. *Expert opinion on therapeutic patents*, 23(9), pp.1133-1156.
26. Keylor, M.H., Matsuura, B.S. and Stephenson, C.R., 2015. Chemistry and biology of resveratrol-derived natural products. *Chemical reviews*, 115(17), pp.8976-9027.
27. Khanam, H., 2015. Shamsuzzaman Bioactive benzofuran derivatives: A review. *Eur. J. Med. Chem*, 97(1), pp.483-504.
28. Naik, R., Harmalkar, D.S., Xu, X., Jang, K. and Lee, K., 2015. Bioactive benzofuran derivatives: Moracins A–Z in medicinal chemistry. *European journal of medicinal chemistry*, 90, pp.379-393.
29. Radadiya, A. and Shah, A., 2015. Bioactive benzofuran derivatives: An insight on lead developments, radioligands and advances of the last decade. *European journal of medicinal chemistry*, 97, pp.356-376.
30. Liang, Z., Xu, H., Tian, Y., Guo, M., Su, X. and Guo, C., 2016. Design, synthesis and antifungal activity of novel benzofuran-triazole hybrids. *Molecules*, 21(6), p.732.
31. Kenchappa, R., Bodke, Y.D., Chandrashekar, A., Telkar, S., Manjunatha, K.S. and Sindhe, M.A., 2017. Synthesis of some 2, 6-bis (1-coumarin-2-yl)-4-(4-substituted phenyl) pyridine derivatives as potent biological agents. *Arabian Journal of Chemistry*, 10, pp.S1336-S1344.
32. Aswathanarayanappa, C., Bheemappa, E., Bodke, Y.D., Bhovi, V.K., Ningegowda, R., Shivakumar, M.C., Peethambar, S.K. and Telkar, S., 2013. 5-phenyl-1-benzofuran-2-

- yl derivatives: synthesis, antimicrobial, and antioxidant activity. *Medicinal Chemistry Research*, 22(1), pp.78-87.
33. Abdel-motaal, M., Kandeel, E. M., Abou-Elzahab, M., & Elghareeb, F. (2017). Synthesis and Evaluation of Antioxidant Activity of Some New Heterocyclic Compounds Bearing the Benzo[B]Furan Moiety. *European Scientific Journal*, ESJ, 13(30), 297-213.
34. Hiremathad, A., Chand, K. and Keri, R.S., 2018. Development of coumarin–benzofuran hybrids as versatile multitargeted compounds for the treatment of Alzheimer's Disease. *Chemical biology & drug design*, 92(2), pp.1497-1503.
35. Thévenin, M., Thoret, S., Grellier, P. and Dubois, J., 2013. Synthesis of polysubstituted benzofuran derivatives as novel inhibitors of parasitic growth. *Bioorganic & medicinal chemistry*, 21(17), pp.4885-4892.
36. Rizzo, S., Rivière, C., Piazzoli, L., Bisi, A., Gobbi, S., Bartolini, M., Andrisano, V., Morroni, F., Tarozzi, A., Monti, J.P. and Rampa, A., 2008. Benzofuran-based hybrid compounds for the inhibition of cholinesterase activity,  $\beta$  amyloid aggregation, and A $\beta$  neurotoxicity. *Journal of medicinal chemistry*, 51(10), pp.2883-2886.
37. Xie, Y.S., Kumar, D., Bodduri, V.V., Tarani, P.S., Zhao, B.X., Miao, J.Y., Jang, K. and Shin, D.S., 2014. Microwave-assisted parallel synthesis of benzofuran-2-carboxamide derivatives bearing anti-inflammatory, analgesic and antipyretic agents. *Tetrahedron Letters*, 55(17), pp.2796-2800.
38. Asif, M., 2016. Mini review on important biological properties of benzofuran derivatives. *J Anal Pharm Res*, 3(2). 48-50.
39. Heravi, M.M., Zadsirjan, V., Hamidi, H. and Amiri, P.H.T., 2017. Total synthesis of natural products containing benzofuran rings. *RSC advances*, 7(39), pp.24470-24521.
40. Kamal, M., Shakya, A.K. and Jawaid, T., 2011. Benzofurans: a new profile of biological activities. *International Journal of Medical and Pharmaceutical Sciences*, 1(3), pp.1-15.
41. Adole, V.A., Pawar, T.B., Koli, P.B. and Jagdale, B.S., 2019. Exploration of catalytic performance of nano-La<sub>2</sub>O<sub>3</sub> as an efficient catalyst for dihydropyrimidinone/thione synthesis and gas sensing. *Journal of Nanostructure in Chemistry*, 9(1), pp.61-76.
42. Adole, V.A., More, R.A., Jagdale, B.S., Pawar, T.B. and Chobe, S.S., 2020. Efficient Synthesis, Antibacterial, Antifungal, Antioxidant and Cytotoxicity Study of 2-(2-Hydrazineyl) thiazole Derivatives. *ChemistrySelect*, 5(9), pp.2778-2786.
43. Adole, V.A., Jagdale, B.S., Pawar, T.B. and Sagane, A.A., 2020. Ultrasound promoted stereoselective synthesis of 2, 3-dihydrobenzofuran appended chalcones at ambient temperature. *South African Journal of Chemistry*, 73, pp.35-43.
44. Lade, J.J., Patil, B.N., Vhatkar, M.V., Vadagaonkar, K.S. and Chaskar, A.C., 2017. An Efficient Synthesis of Pyrrolo [1,2-a] quinoxalines by Copper-Catalyzed C–H Activation of Arylacetic Acids. *Asian Journal of Organic Chemistry*, 6(11), pp.1579-1583.
45. Patil, B.N., Sathe, P.A., Parade, B.S., Vadagaonkar, K.S. and Chaskar, A.C., 2018. Transition metal free one pot synthesis of aryl carboxylic acids via dehomologative oxidation of styrenes. *Tetrahedron letters*, 59(49), pp.4340-4343.
46. Adole, V.A., Jagdale, B.S., Pawar, T.B. and Sawant, A.B., Experimental and theoretical exploration on single crystal, structural, and quantum chemical parameters of (E)-7-(arylidene)-1,2,6,7-tetrahydro-8H-indeno [5,4-b] furan-8-one derivatives: A comparative study. *Journal of the Chinese Chemical Society*. <https://doi.org/10.1002/jccs.202000006>.
47. Patil, M.P., Singh, R.D., Koli, P.B., Patil, K.T., Jagdale, B.S., Tipare, A.R. and Kim, G.D., 2018. Antibacterial potential of silver nanoparticles synthesized using Madhuca longifolia flower extract as a green resource. *Microbial pathogenesis*, 121, pp.184-189.
48. Shinde, S.G., Patil, M.P., Kim, G.D. and Shrivastava, V.S., 2020. Ni, C, N, S multi-doped ZrO<sub>2</sub> decorated on multi-walled carbon nanotubes for effective solar induced degradation of anionic dye. *Journal of Environmental Chemical Engineering*, 8(3), p.103769.
49. Lade, J.J., Patil, B.N., Vadagaonkar, K.S. and Chaskar, A.C., 2017. Oxidative cyclization of amidoximes and thiohydroxamic acids:

- A facile and efficient strategy for accessing 3, 5-disubstituted 1, 2, 4-oxadiazoles and 1, 4, 2-oxathiazoles. *Tetrahedron Letters*, 58(22), pp.2103-2108.
50. Chaudhari, M.B., Jayan, K. and Gnanaprakasam, B., 2020. Sn-Catalyzed Criegee-Type Rearrangement of Peroxyoxindoles Enabled by Catalytic Dual Activation of Esters and Peroxides. *The Journal of Organic Chemistry*, 85(5), pp.3374-3382.
51. Koli, P.B., Kapadnis, K.H., Deshpande, U.G. and Patil, M.R., 2018. Fabrication and characterization of pure and modified Co<sub>3</sub>O<sub>4</sub> nanocatalyst and their application for photocatalytic degradation of eosine blue dye: a comparative study. *Journal of Nanostructure in Chemistry*, 8(4), pp.453-463.
52. Shinde, S.G., Patil, M.P., Kim, G.D. and Shrivastava, V.S., 2019. Multi-doped ZnO photocatalyst for solar induced degradation of indigo carmine dye and as an antimicrobial agent. *Journal of Inorganic and Organometallic Polymers and Materials*, pp.1-12.
53. Koli, P.B., Kapadnis, K.H. and Deshpande, U.G., 2019. Transition metal decorated Ferrosiferic oxide (Fe<sub>3</sub>O<sub>4</sub>): An expeditious catalyst for photodegradation of Carbol Fuchsin in environmental remediation. *Journal of Environmental Chemical Engineering*, 7(5), p.103373.
54. Adole, V.A., Synthetic approaches for the synthesis of dihydropyrimidinones/ thiones (biginelli adducts): a concise review. 9 (6) 1067-1091.
55. Adole, V.A., Waghchaure, R.H., Jagdale, B.S. and Pawar, T.B., 2020. Investigation of Structural and Spectroscopic Parameters of Ethyl 4-(4-isopropylphenyl)-6-methyl-2-oxo-1,2,3,4-tetrahydropyrimidine-5-carboxylate: a DFT Study. *Chemistry & Biology Interface*, 10(1), 22-20.
56. Sawant, A.B. and Wagh, S.G., 2018. Density, viscosity, DFT and FTIR study of tertiary butyl alcohol and ethanol with DMSO and DMF at room temperature. *Indian Journal of Pure & Applied Physics (IJPAP)*, 56(5), pp.405-414.
57. Pawar, T.B., Jagdale, B.S., Sawant, A.B. and Adole, V.A., 2017. DFT Studies of 2-[(2-substitutedphenyl) carbamoyl] benzoic acids. *Journal of Chemical, Biological and Physical Sciences*, 7, pp.167-175.
58. Seyedkatouli, S., Vakili, M., Tayyari, S.F., Hansen, P.E. and Kamounah, F.S., 2019. Molecular structure and intramolecular hydrogen bond strength of 3-methyl-4-amino-3-penten-2-one and its NMe and N-Ph substitutions by experimental and theoretical methods. *Journal of Molecular Structure*, 1184, pp.233-245.
59. Adole, V.A., Waghchaure, R.H., Jagdale, B.S., Pawar, T.B. and Pathade, S.S., Molecular structure, frontier molecular orbital and spectroscopic examination on dihydropyrimidinones: a comparative computational approach. *Journal of Advanced Scientific Research*, 2020. 11 (2), pp.64-70.
60. Selvaraj, S., Rajkumar, P., Kesavan, M., Thirunavukkarasu, K., Gunasekaran, S., Devi, N.S. and Kumaresan, S., 2020. Spectroscopic and structural investigations on modafinil by FT-IR, FT-Raman, NMR, UV-Vis and DFT methods. *Spectrochimica Acta Part A: Molecular and Biomolecular Spectroscopy*, 224, p.117449.
61. Balakrishnan, A., Sambanthan, M., Murugesan, R. and Sundaram, S., 2020. Molecular structure, spectroscopic (FT-IR, FT-Raman, NMR, UV-VIS), chemical reactivity and biological examinations of Ketorolac. *Journal of Molecular Structure*, p.128040.
62. Manjusha, P., Muthu, S. and Raajaraman, B.R., 2020. Density functional studies and spectroscopic analysis (FT-IR, FT-Raman, UV-visible, and NMR) with molecular docking approach on an antifibrotic drug Pirfenidone. *Journal of Molecular Structure*, 1203, p.127394.
63. Simbizi, R., Gahungu, G. and Nguyen, M.T., 2020. Molecular structure, IR, Raman and UV-VIS spectra of 2-cyanothiophene and 3-cyanothiophene: A comparative quantum chemical investigation. *Spectrochimica Acta Part A: Molecular and Biomolecular Spectroscopy*, p.118393.
64. Frisch, M., Frisch, M., Trucks, G., Schlegel, K.H., Scuseria, G., Robb, M.A., Cheeseman, J., Montgomery, J., Vreven, T., Kudin, K.N. and Burant, J., 2004. Gaussian 03, revision D. 02.